ISSN 0006-3509, Biophysics, 2015, Vol. 60, No. 3, pp. 449–456. © Pleiades Publishing, Inc., 2015.
Original Russian Text © A.V. Kolobov, M.B. Kuznetsov, 2015, published in Biofizika, 2015, Vol. 60, No. 3, pp. 555–563.

BIOPHYSICS OF COMPLEX SYSTEMS

# Investigation of the Effects of Angiogenesis on Tumor Growth Using a Mathematical Model

**A. V. Kolobov[a, b] and M. B. Kuznetsov[a]**

[a] *Lebedev Physical Institute, Russian Academy of Sciences, Leninskii pr. 53, Moscow, 119991 Russia*
[b] *Institute of Numerical Mathematics, Russian Academy of Sciences, ul. Gubkina 8, Moscow, 119333 Russia*
*e-mail: kolobov@lpi.ru*

Received December 8, 2014

**Abstract**—A mathematical model of tumor growth has been developed that takes angiogenesis into account. Malignant cells under metabolic stress produce vascular endothelial growth factor, which stimulates angiogenesis and, thus, increases nutrient influx into a tumor. The model takes into account migration-proliferation dichotomy in malignant cells that depends on the nutrient concentration. Convective fluxes that occur upon active tumor-cell proliferation in a compact dense tissue have been also considered. The computational investigation of the model demonstrated that the diffusive tumor growth rate does not depend on angiogenesis, while for noninvasive tumors angiogenesis could significantly alter tumor growth, although it is not able to stop it completely. The causes and significance of the results for the estimation of the antitumor efficacy of antiangiogenic therapy are discussed.

*Keywords*: mathematical simulation, tumor, angiogenesis
**DOI:** 10.1134/S0006350915030082

Over the recent decades, the fight against oncological diseases in developed countries has become one of the key factors in the development of medicine and medical and biological research. One of the promising directions of treatment is considered to be antitumor antiangiogenic therapy (AAT). In 1966 J. Folkman et al. demonstrated that the preexisting blood–vascular system provides the growth of a tumor xenograft in an isolated organ up to a radius of 3–4 mm [1], while further growth requires neovascularization, i.e., formation of new blood vessels from the preexisting vascular network. The antiangiogenic therapy suggested by Folkman in 1971 [2] is aimed at limitation of the influx of nutrients into a tumor by blocking tumor angiogenesis.

At present, a great number of different factors that both stimulate and inhibit tumor neovascularization are known [3]. Nevertheless, the most universal mediator of angiogenesis is considered to be the vascular endothelial growth factor (VEGF). This molecule, which weighs 34–42 kDa depending on its isoform, interacts with the receptors on the membrane of an endothelial cell converting it to its active state. The activated cell can differentiate in two directions, obtaining either a migration or proliferation phenotype. Cells with a migration phenotype, which constitute the tip of a capillary that is being formed, choose the direction of its growth via filopodia. It is believed that the growth occurs predominantly along a gradient of oxygen decrease. At the same time, cells with a proliferation phenotype, which are located in a capillary trunk, are responsible for its elongation.

Neovascularization takes place not only during tumor growth, but also upon wound healing, postsurgical recovery of tissues, and pregnancy. However, a significant difference of the capillary network that forms during tumor angiogenesis from the one that preexists in a tissue or those that form as a result of other types of neovascularization is its inefficiency [4]. The vascular network that forms as a result of tumor angiogenesis has an irregular structure with a great number of blind capillaries; the newly formed capillaries themselves have a greater diameter, numerous large pores in their walls, and decreased blood content, when compared to the preexisting capillaries. Moreover, during their growth, tumor cells produce different enzymes, in particular, EphB4, which disturb angiogenesis regulation, which leads to degradation of most capillaries within the tumor and thickening of the walls of the remaining ones, thus preventing the penetration of nutrients into the tissue [5].

All these issues lead to natural questions: how does tumor angiogenesis accelerate the growth of the tumor and how does it depend on its type and/or localization? This question is fundamental for the evaluation of the potential effectiveness of AAT for a certain patient. In clinical practice, it is possible only to

Abbreviations used: AAT, antitumor antiangiogenic therapy; VEGF, vascular endothelial growth factor.

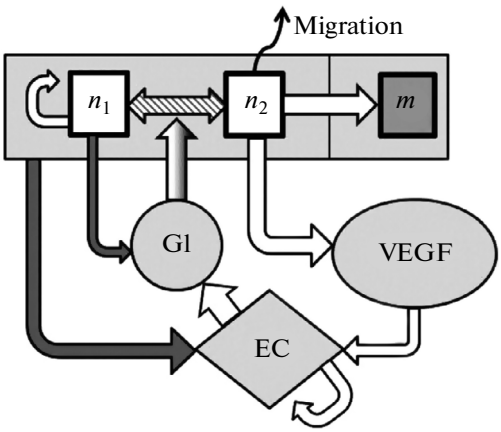


**Fig. 1.** A block diagram of the model. $n_1$, $n_2$, and $m$, proliferating, migrating, and dead cells of a tumor, respectively; Gl, glucose; VEGF, vascular endothelial growth factor; EC, density of the vascular network. The white arrows show activating connections; the dark arrows show inhibiting connections.

observe the results of using AAT [6–8]. The prediction of its antitumor effectiveness beforehand using mathematical simulation could be attempted.

The main difficulty in the simulation of tumor growth considering angiogenesis is the problem of taking processes with different scales into account. In fact, the capillary diameter is 5–10 μm; the distance between capillaries is 100–200 μm; the average length of the capillary is 0.5–1.0 mm; and the tumor size can reach tens of centimeters, i.e., the scale difference is four orders of magnitude. To simulate the growth of individual capillaries and interactions of cells with each other and the environment, cellular automaton models are mainly used [9, 10]. However, models of this type require extremely long computations, even when calculating regions with sizes of approximately 1 cm. It should be noted that in the first works on angiogenesis simulation tumor growth was not taken into account and the tumor was considered as a stationary source of VEGF [11, 12]. To simulate tumor growth, continuous models are more suitable with the tumor and its surroundings being described by cell densities and concentrations of substances [13–17]. Here, it is a great challenge to correctly describe the transport of nutrients in the capillary network; owing to this, the problem of the correct relationship in the model between micro- and macroprocesses is urgent [18].

It should be admitted that continuous models in the literature contain a great number of parameters, many of which almost can not be determined experimentally, which decreases their forecasting power for the evaluation of the antitumor effectiveness of antiangiogenic therapy. In these studies, the results of simulation are only qualitatively compared with the data of magnetic resonance tomography and histological studies of clinical patients. Although this comparison demonstrates the qualitative agreement of the spatial structure of a real tumor and the results of a simulation, the practical value of this approach is doubtful.

We have developed a continuous mathematical model of the growth of an invasive tumor that takes angiogenesis into account [19]. This model considers the densities of tumor cells of different types, the concentrations of nutrients and VEGF, and the density of the vascular network in the tissue. Using this approach, the main problem is accounting for the change in the influx of nutrients due to remodeling of the vascular network. Solving this problem depends on the choice of the nutrient in the model. The influx of oxygen, whose content significantly differs in arterial and venous blood, depends on the volume of the blood that runs through the tissue. Due to this, upon choosing oxygen as a key metabolite, the relationship between the influx and density of the vascular network is not obvious and requires a distinct study. In the case where glucose is chosen as the key metabolite, the picture is simpler. Since the glucose concentrations in arterial and venous blood differ little (even in brain vessels this difference is about 12%), the influx to the tissue is proportional to the surface area of the tissue capillaries. In this case, the density of the vascular network is linearly connected with the influx of the nutrient, which we used during the simulation. The development of experimental methods of this study makes it possible to perform a detailed angiography of a capillary network and to obtain data on its density, including its surface density in different tumor regions [20].

The results of our simulation [19] revealed that angiogenesis does not affect the growth of an invasive tumor; thus, AAT is not effective against the tumor. However, in the model we took only the random motility of tumor cells into account and ignored convective fluxes that occur upon tumor growth in a compact dense tissue. As demonstrated in [21], it is these fluxes that determine the growth rate of a low-invasive tumor. Thus, in this study a model of tumor growth that takes angiogenesis into account has been considered, which factors in both the intrinsic motility of the malignant cells and convection in the tissue. From the practical point of view, this simulation will make it possible to evaluate the potential antitumor effectiveness of AAT both for high- and low invasive tumors.

## MODEL

The interaction of the variables in a model of tumor growth with angiogenesis is given in Fig. 1.

This model considers a tumor as a cell colony that is surrounded by normal tissue with a preexisting vascular network. Living tumor cells can be in two states: a proliferating one with the density $n_1(r, t)$ and a migrating one with the density $n_2(r, t)$, where $r$ is the spatial coordinate and $t$ is the time. The intensity of the

transition from one state to another one $P_1(S)$, $P_2(S)$ depends on the concentration of the nutrient $S(r, t)$. At its high concentration, the cells divide at the constant rate $B$ and do not diffuse. When the metabolite concentration significantly decreases, the cells stop dividing and begin to migrate randomly with the coefficient $D_n$ searching for regions with a high level of the nutrient. If the migrating cells do not reach a region with a high concentration of the nutrient, they die at the rate $d_n$. The density of the dead cells is $m(r, t)$. We have already used this approach in a previous work on the simulation of the growth of an invasive tumor [21]. It is based on the principle of migration-proliferation dichotomy of tumor cells that is observed experimentally [23]. Along with tumor cells, the model considers the normal cells of the organism, $h(r, t)$. It is believed that they do not divide and do not possess intrinsic motility. Under the effects of factors released by active tumor cells, they die at the rate $H(n_1 + n_2)$, where $H$ is the lysis parameter. We consider a compact dense tissue so that $h(r, t) + n_t(r, t) = \text{const}$, where $n_t(r, t)$ is the total density of the tumor cells, including the dead cells $n_t(r, t) = n_1(r, t) + n_2(r, t) + m(r, t)$. We assume that the volumes of all the cells are identical. Taking convection into account, with $I(r)$ being the rate of the convective flux, the equations for all the cells in the model in a one-dimensional case are as follows

$$\begin{aligned}
\frac{\partial n_1}{\partial t} &= Bn_1 - P_1(S)n_1 + P_2(S)n_2 - \frac{\partial (I(x)n_1)}{\partial x},\\
\frac{\partial n_2}{\partial t} &= D_n\frac{\partial^2 n_2}{\partial x^2} + P_1(S)n_1 - P_2(S)n_2\\
&\quad - d_n n_2 - \frac{\partial (I(x)n_2)}{\partial x},\\
\frac{\partial m}{\partial t} &= d_n n_2 - \frac{\partial (I(x)m)}{\partial x},\\
\frac{\partial h}{\partial t} &= -H(n_1 + n_2)h - \frac{\partial (I(x)h)}{\partial x}.
\end{aligned} \tag{1}$$

Since the total density of the normal and tumor cells is constant, then taking it as unity we exclude the equation for the normal cells from the system and obtain the expression for the potential component of the velocity of the convective flux $U(x) = \int_0^x [Bn_1 - H(n_1 + n_2)(1 - n_1)]dr$. The derivation of this equation was described in [24]. Here, we assume that stresses that occur in the tissue are transmitted simultaneously; this is justified by the fact that their relaxation time is small compared with the time of cell division.

Then, the system of equations for the cell densities could be written as

$$\begin{aligned}
\frac{\partial n_1}{\partial t} &= Bn_1 - P_1(S)n_1 + P_2(S)n_2 - \frac{\partial (I(x)n_1)}{\partial x},\\
\frac{\partial n_2}{\partial t} &= D_n\frac{\partial^2 n_2}{\partial x^2} + P_1(S)n_1 - P_2(S)n_2\\
&\quad - d_n n_2 - \frac{\partial (I(x)n_2)}{\partial x},\\
\frac{\partial m}{\partial t} &= d_n n_2 - \frac{\partial (I(x)m)}{\partial x},\\
I(x) &= D_n\frac{\partial n_2}{\partial x} + U(x) = D_n\frac{\partial n_2}{\partial x}\\
&\quad + \int_0^x [Bn_1 - H(n_1 + n_2)(1 - n_t)]dr,\\
P_1(S) &= k_1\exp(-k_2 S),\\
P_2(S) &= k_3(1 - \tanh[(S_{\text{crit}} - S)\varepsilon]).
\end{aligned} \tag{2}$$

The form of the functions $P_1(S)$ and $P_2(S)$ is of importance. The intensity of the transition from proliferation to migration $P_1(S)$ was taken from [25], where it was successfully used for fitting experimental data. The parameter $k_1$ describes the maximal intensity of the transition, and $k_2$ characterizes the sensitivity to a shortage of the nutrient. Unfortunately, there are no experimentally proven data on the form of the function $P_2(S)$. Therefore, we used a smooth function that is close to a step one, where $S_{\text{crit}}$ is the concentration of the nutrient exceeding which causes the cell to stop migrating and begin dividing, $2k_3$ is the maximal intensity of the transition from migration to proliferation, and $\varepsilon$ describes the difference of the function $P_2(S)$ from the step one: $P_2(S) = 2k_3\Theta(S - S_{\text{crit}})$ at $\varepsilon \to 0$. We have used this form of the transition function already for the simulation of the growth of an invasive tumor considering migration-proliferation dichotomy of its cells [22].

The nutrient is delivered by the vascular network, diffuses throughout tissue, and is consumed by both malignant cells (the proliferating cells consume it in significantly larger amounts than the migrating ones do) and normal cells.

The model considers the averaged characteristic of the vascular network in the tissue, namely, its density. The reasons for this were discussed in detail in the Introduction. We believe that initially in the tissue a capillary network that is sufficient for vital functions of the tissue exists; its density is taken as unity. Here, the vascular system can become denser as a result of angiogenesis depending on the concentration of vascular endothelial growth factor (VEGF), which is $V(r, t)$. The capillaries inside the tumor are destroyed.

The VEGF distribution in the tissue is determined by the balance of its production by the tumor cells, diffusion, nonspecific degradation, and utilization by the endothelial cells that constitute the vascular system. Thus, the equations for the nutrient concentration, the density of the vascular network in the tissue, and the concentration of the proangiogenic factor are the following

$$\begin{aligned}\frac{\partial S}{\partial t} &= D_s\frac{\partial^2 S}{\partial x^2} - \frac{q_t(n_1 + Kn_2)S}{S + S^*} - \frac{q_h(1 - n_t)S}{S + S^*} + Q_0 EC,\\ \frac{\partial EC}{\partial t} &= \frac{RV}{V + V^*}EC(1 - EC/EC_{\max}) - ln_t EC,\\ \frac{\partial V}{\partial t} &= D_V\frac{\partial^2 V}{\partial x^2} + p(fn_1 + n_2) - d_V V - \omega VEC,\end{aligned} \quad (3)$$

where $D_s$ is the diffusion constant of the substrate, $q_t$ is the rate of consumption of the substrate by the tumor, $K$ is a parameter that determines the difference in the intensity of the consumption of the nutrient by the migrating and dividing cells, $S^*$ limits the cell consumption of the nutrient at its low concentrations, $q_h$ is the coefficient of consumption of the substrate by the normal tissue, and $Q_0$ is a parameter that determines its influx from the vessels, the density of which in the tissue is specified by the variable $EC(r, t)$. It is chosen so that in the absence of a tumor in a tissue with the preexisting vascular system $EC_0 = 1$ the constant level of the nutrient $S(r, t) = 1$ is maintained. $R$ is the maximal rate of vessel growth; $l$ is the rate of degradation of the vascular network inside the tumor; $D_V$ is the diffusion constant of VEGF; $p$ is the rate of VEGF production by the migrating tumor cells; $f$ is the ratio of the rates of its production by different types of malignant cells; $d_V$ is the rate of VEGF nonspecific degradation; and $\omega$ is the rate of its utilization by the endothelial cells of the vascular network during angiogenesis. It should be emphasized that the model uses only non-negative parameters.

The system of equations (2), (3) makes it possible to simulate both the tumor growth depending on the influx of nutrients through the vascular network into the tissue and the change in this network induced by the tumor growth.

## RESULTS

It is well known that at the initial stage of growth a tumor is spherical. With an increase in its radius up to several millimeters, a necrotic region is formed in the center of the tumor, with living cells being absent. Since differences in the Laplace operator in the spherically symmetrical and planar cases are significant only for small radii, then the use of planar geometry for simulating tumors with a central necrotic region does not lead to any significant distortion of the result. Thus, system of equations (2), (3) was solved in a one-dimensional plane region with the size $L = 2$ (cm) on the assumption that at the left boundary there is the center of the tumor, which grows to the right towards the normal tissue with the preexisting vascular network. Thus, the boundary conditions will be the following:

$$\begin{cases} n_{1x}(0, t) = 0, \\ n_{2x}(0, t) = 0, \\ m_x(0, t) = 0, \\ S_x(0, t) = 0, \\ EC_x(0, t) = 0, \\ V_x(0, t) = 0, \end{cases} \quad \begin{cases} n_1(L, t) = 0, \\ n_2(L, t) = 0, \\ m(L, t) = 0, \\ S(L, t) = 1, \\ EC(L, t) = 1, \\ V_x(L, t) = 0. \end{cases} \quad (4)$$

The model contains a great number of parameters, with the values being taken predominantly from the literature data. Lewis lung carcinoma was chosen as the basic tumor type. This is a well-known tumor that has high metastatic potential and thus is highly invasive. In [25], the main kinetic parameters of this tumor cell type are given. The critical metabolite in this study was represented by glucose rather than oxygen. Thus, we also chose glucose as a nutrient in the model. This is acceptable for a qualitative study, since the regions of hypoxia and hypoglycemia (shortages of oxygen and glucose, respectively) almost coincide in a tumor [26]. Moreover, in [25] the rate of VEGF production by tumor cells under metabolic stress was assessed. The greatest problems were connected with determination of the values of the equation parameters for the density of the vascular network (2), since this equation describes several averaged characteristics. The primary estimate of the maximal growth rate of the vascular network density, $R$, was taken from [27]. The other parameters of the model were chosen from a physiologically reasonable range so as to reproduce the known structure of a tumor in the tissue. The parameter of the lysis of the normal cells was assessed according to the consideration that their death rate should be much less than the rate of degradation of the vascular network within the tumor, since in reality cell death is connected with the release of the substances that constitute it and in our model the cell simply disappears, emptying the space for tumor cells. The other parameters that determine the VEGF dynamics in the tissue were taken from the study of Milde et al. [28].

For the convenience of calculations, all the parameters were made nondimensional. The normalization values were chosen as the following: for the time—$t_0 =$ 1 h, for the length—$L_0 = 10^{-2}$ cm, for the cell density—$n_{\max} = 108$ cells/mL, for the glucose concentration—$S_0 = 1$ mg/mL, and for the VEGF concentration—$V_0 = 10^{-13}$ mol/mL. As mentioned, the normal vascular density in the tissue was taken as unity—$EC_0 = 1$. After making the parameters nondimen-

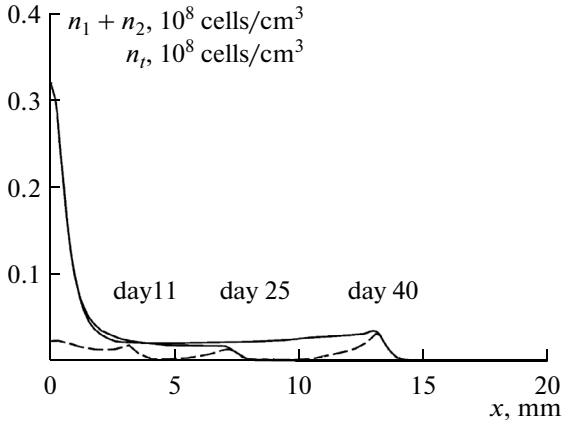


**Fig. 2.** The spatial distribution of the total density $n_t = n_1 + n_2 + m$ (solid line) and the density of living cells $n_1 + n_2$ (dashed line) of an invasive tumor on the 11th, 25th, and 46th days of the growth for the standard set of parameters.

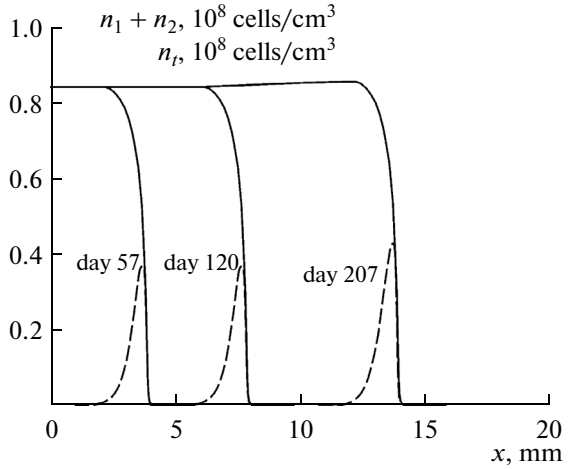


**Fig. 3.** The spatial distribution of the total density $n_t = n_1 + n_2 + m$ (solid line) and the density of living cells $n_1 + n_2$ (dashed line) of a noninvasive tumor on the 57th, 120th, and 207th days of the growth for a standard set of parameters.

sional, the following set of parameters was chosen as basic:

$$L = 200, \quad B = 0.047, \quad d_n = 0.01,$$
$$D_S = 108, \quad q_t = 5.1, \quad K = 0.025,$$
$$S^* = 0.02, \quad q_n = 0.1275, \quad Q_0 = 0.125,$$
$$D_V = 21.6, \quad p = 20, \quad f = 0,$$
$$d_V = 0.1, \quad \omega = 1, \quad R = 0.0075,$$
$$V^* = 0.1, \quad EC_{\max} = 3, \quad l = 1,$$
$$H = 0.01, \quad k_1 = 0.4, \quad k_2 = 19.8,$$
$$k_3 = 0.12, \quad S_{\text{crit}} = 0.3, \quad \varepsilon = 10.$$

Using this set of parameters, computational investigation of the model was performed for two values of the diffusion of the malignant cells, $D_i = 0.36$ and $D_c = 0.0036$. The first coefficient in dimensional units is $D_i = 10^{-8}$ cm$^2$/s; this is a large value, which is usually assigned to metastatic high invasive tumor types, for example, gliomas [15]. These tumors grow mainly due to intrinsic cell motility and the effect of convection is small. The other value of the diffusion constant of $D_c = 10^{-12}$ cm$^2$/s corresponds to low-invasive tumors. This tumor is much denser and convection is of great importance for its growth.

At the initial moment of time $t = 0$, it was assumed in the entire region that $S(x, 0) = 1$, $EC(x, 0) = 1$, $V(x, 0) = 0$, $n_2(x, 0) = m(x, 0) = 0$, and a small population of proliferating tumor cells is near the left boundary of the region $n_1(x, 0) = 0.5 - 0.02x^2$ at $x \le 5$ and $n_1(x, 0) = 0$ at $x > 5$.

For a numerical solution of the system (2), (3), the method of splitting with respect to physical processes was used. The convection equations were solved via the Lax–Wendroff method; the kinetic equations were solved by the Runge–Kutta method and the Crank–Nicolson method was used to solve the diffusion equations.

The results of the model calculations for the standard set of parameters at the different diffusions are given in Figs. 2–5. As can be seen from these plots, the results of the simulation reproduce the tumor structure correctly, with a layer of active cells at the boundary and a necrotic region in the center of the tumor. Here, at the boundary of the tumor and normal tissue an increased density of the vascular network is observed, while there are almost no vessels inside the tumor.

As can be seen from Figs. 2 and 3, the low-invasive tumor is denser compared to the invasive one, which was mentioned earlier. For a difference in the diffusion constants by two orders of magnitude, the radius of the invasive tumor increases almost five times faster.

The difference between high and low-invasive tumors is also manifested in the shape of their front boundaries, with that of the high-grade invasive tumor being fuzzier.

Figures 4 and 5 clearly demonstrate that in the low invasive tumor angiogenesis is more intense, with the vascular network at the tumor boundary becoming denser by a factor of more than 2.5, whereas in the high-invasive tumor this increase is insignificant. The difference in the intensity of the angiogenesis is also indicated by VEGF, the peak value of which for the low-invasive tumor is higher by a factor of 15–20.

A key question that should be answered by our study is how strongly angiogenesis affects the tumor growth rate at different motilities of its cells. For this, we varied two parameters in the equation for the density of the vascular network (3), $R$ and $l$. It should be emphasized that both parameters were varied within a

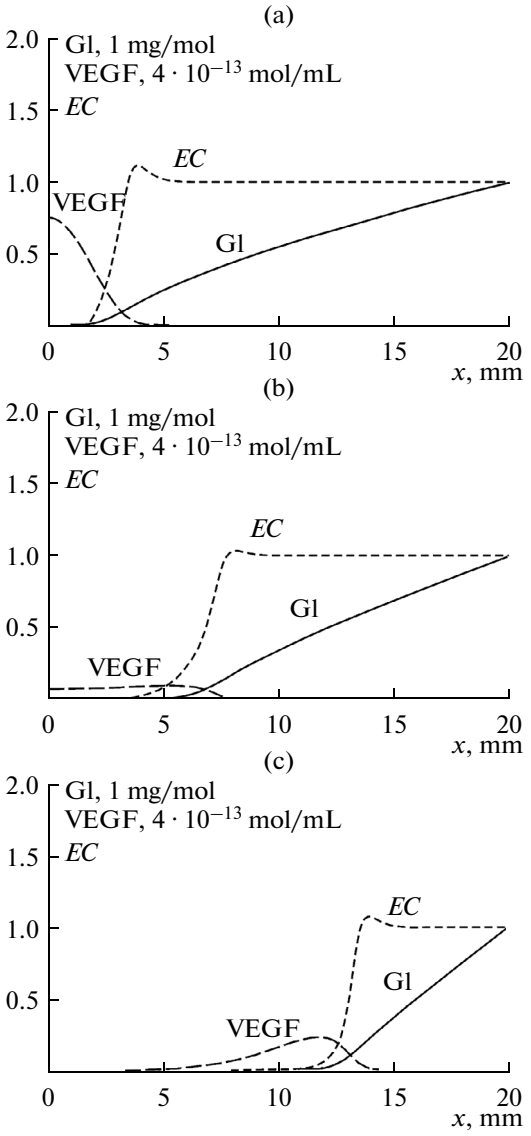


**Fig. 4.** The spatial distribution of glucose (Gl) (solid line), VEGF concentrations (large dashed line), and the density of the vascular network in the tissue *EC* (small dashed line) on the 11th (a), 25th (b), and 46th (c) days of the growth of an invasive tumor for a standard set of parameters.

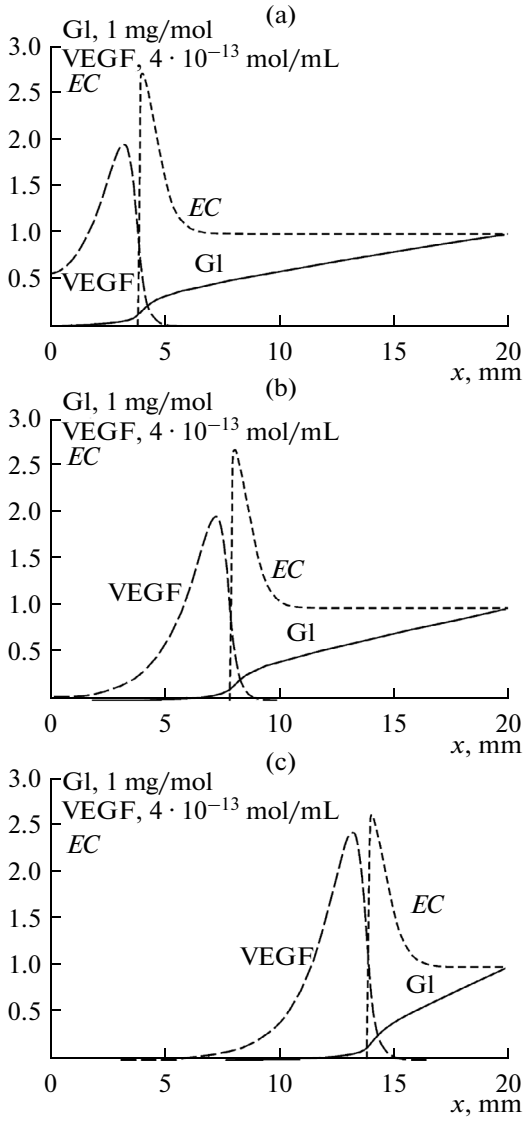


**Fig. 5.** The spatial distribution of glucose (Gl) (solid line), VEGF concentrations (large dashed line), and density of the vascular network in the tissue *EC* (small dashed line) on the 57th (a), 120th (b), and 207th (c) days of the growth of a non-invasive tumor for the standard set of parameters.

very wide range, $R \in [0.0015, 0.015]$ and $l \in [0.05, 10]$. Here, the maximal value $R = 0.015$ corresponds to doubling of the density of the vascular network in 4 days (at high VEGF concentration), which is near the limit of the physiologically possible values for the angiogenesis rate. A zero value of the rate of degradation of the vascular network by the tumor $l = 0$ is not acceptable, since in this case there are sources of nutrients and, thus, active cells inside the necrotic region of the tumor, which is not observed in experiments. Histological data indicate that even if there is a vessel inside a tumor, the high thickness of its walls prevents an influx of nutrients from the blood into the tissue. Figure 6 gives the time dependence of the radius of the invasive tumor for the different values $R$ and $l$. The radius was chosen as the maximal value of $x$, for which $n_1(x, t) + n_2(x, t) > 0.001$. As can be seen from the plots, the growth rate of the invasive tumor does not depend on the parameters that determine the rate of remodeling of the vascular network; in the case of a noninvasive tumor this dependence exists (Fig. 7).

## CONCLUSIONS

In this study a continual multicomponent model of the growth of a vascularized tumor was created, which considered not only the intrinsic motility of malignant cells, but also the convective fluxes that occur during

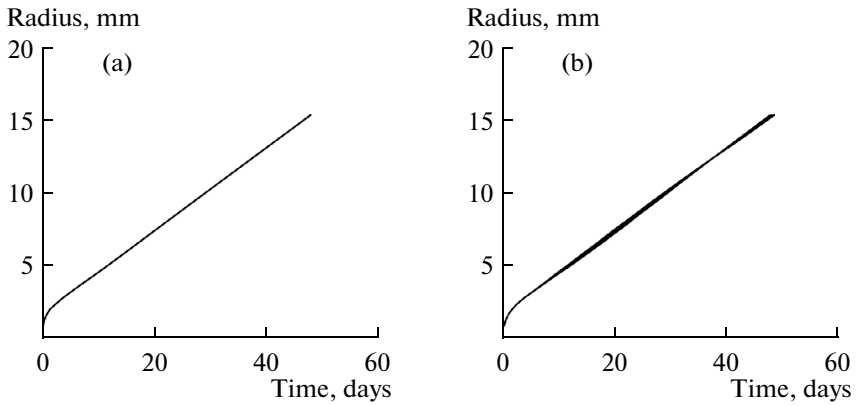


**Fig. 6.** The time dependences of the size of an invasive tumor upon variation of the parameters of the vascular network, maximal growth rate $R$ (a), and vascular network degradation rate within the tumor $l$ (b). The parameters were varied by turns $R = 0.0015$, 0.002, 0.0025, 0.005, 0.0075, 0.01, 0.015 and $l = 0.05$, 0.1, 0.5, 1, 2.5, 5, 10. The remaining parameters were from the standard set.

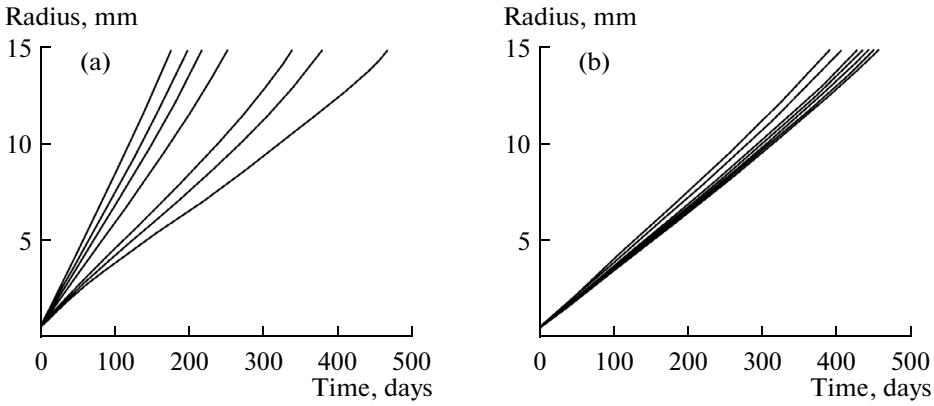


**Fig. 7.** The time dependences of the size of a noninvasive tumor upon variation of parameters of the vascular network, maximal growth rate $R$ (a), and vascular network degradation rate within the tumor $l$ (b). The parameters were varied by turns $R = 0.0015$, 0.002, 0.0025, 0.005, 0.0075, 0.01, 0.015 and $l = 0.05$, 0.1, 0.5, 1, 2.5, 5, 10. The remaining parameters were from the standard set.

tumor growth in a compact dense tissue. It was assumed in the model that the invasive tumors are characterized by high cell motility, whereas the low-invasive tumors grow predominantly due to the convective fluxes in the tissue. The results of the simulation revealed that in the case of the low-invasive tumor angiogenesis significantly increases the rate of the tumor's growth. This is not surprising, since the convection at the tumor boundary that determines the rate of its growth depends on the total proliferation of its cells inside, which grows up with an increase in the influx of nutrients during angiogenesis. Thus, it could be concluded that in the case of a low-invasive tumor angiogenic therapy could have a significant antitumor effect; however, even in the absence of angiogenesis, when the density of the vascular network almost does not increase, the tumor growth does not stop completely. We previously demonstrated that angiogenesis does not affect the growth rate of a tumor that grows only due to the cell migration [19]. However, taking convection into account could have influenced this result if the rates of the convective and diffusive growth added together. Nevertheless, high activity of proteolytic enzymes near the tumor, which is observed in experiments and is taken into account in our model, induces the death of normal cells behind the growth front of the high-invasive tumor. This leads to a decrease in the convective flux at its boundary. Moreover, the convection rate at the front of an invasive tumor may be directed toward the tumor center, which would lead to the slowing of its increase. Thus, taking tissue convection into account does not change the key result: the growth rate of an invasive tumor almost does not depend on angiogenesis and, thus, AAT would not have an antitumor effect.

At present, a sufficient amount of experimental data on the clinical application of antitumor angiogenic therapy that employs bevacizumab (monoclonal antibody to VEGF) has been accumulated [7, 29, 30]. These data are ambiguous, since for some tumors AAT appears to be effective and for others it does not. The present study at least gives one of the possible explana-

tions of such results and agrees with the clinical data. Unfortunately, in most cases the clinical classification of malignant tumors does not make it possible to unequivocally determine which of the transport processes in the tissue, cell motility or convection fluxes, defines the tumor growth. In our opinion this is the reason that the clinical data on the effectiveness of AAT seem ambiguous in most cases [30]. However, if the clinical type of the tumor makes it possible to determine the character of its growth sufficiently clearly, then our conclusions are supported by the experimental data. Indeed, metastatically active pancreatic cancer cells have high motility; thus, according to our model AAT would be ineffective in their case, which is observed in clinics [29]. In the case of non-small cell lung carcinoma, it is reasonable to suggest that tissue convection plays a more important role than the cell motility; thus, AAT would be effective, which is also shown by the clinical data [7].

## ACKNOWLEDGMENTS

This study was supported by the Russian Science Foundation, project no. 14-31-00024.

## REFERENCES

1. J. Folkman, P. Cole, and S. Zimmerman, Ann. Surg. **164**, 491 (1966).
2. J. Folkman, N. Engl. J. Med. **285**, 1182 (1971).
3. T. H. Adaír and J.-P. Montani, *Angiogenesis*, Ed. by J. Granger and D. N. Granger, in Morgan and Claypool Life Sciences Series (San Rafael, 2011).
4. M. A. Konerding, C. van Ackern, and E. Fait, in *Blood Péfusion and Microenvironment of Human Tumors: Implications for Clinical Radiooncology*, Ed. by M. Molls and P. Vaupel (Springer, Berlin, 2002), pp. 5–17.
5. M. Welter, K. Bartha, and H. Rieger, J. Theor. Biol. **259**, 405 (2009).
6. T. Deng, L. Zhang, X.-J. Liu, et al., Med. Oncol. **30** (4), (2013).
7. G. Dranitsaris, N. Beegle, A. Ravelo, et al., Clin. Lung Cancer **14** (2), 120 (2013).
8. M. Nishino, A. Giobbie-Hurder, N. H. Ramaiya, and F. S. Hodi, J. Immunother. Cancer **2** (1), (2014).
9. J. Wang, L. Zhang, C. Jing, et al., Theor. Biol. Med. Model. **10** (2013).
10. M. Welter, K. Bartha, and H. Rieger, J. Theor. Biol. **250**, 257 (2007).
11. N. V. Mantzaris, S. Webb, and H. G. Othmer, J. Math. Biol. **49**, 111 (2004).
12. A. Stephanou, S. R. McDougall, A. R. A. Anderson, and M. A. J. Chaplain, Math. Comput. Model. **44**, 96 (2006).
13. M. C. Eisenberg, Y. Kim, R. Li, et al., Proc. Natl. Acad. Sci. U. S. A. **180** (50), 20078 (2011).
14. P. Hinov, P. Gerlee, L. J. McCavley, et al., Math. Biosci. Eng. **6**, 521 (2009).
15. K. R. Svanson, R. C. Rockne, J. Claridge, et al., Cancer Res., **71**, 7366 (2011).
16. B. Szomolay, T. D. Eubank, R. D. Roberts, et al., J. Theor. Biol. **303**, 141 (2012).
17. M. Welter and H. Rieger, Eur. Phys. J. E **33**, 149 (2010).
18. F. Spill, P. Guerrero, T. Alarcon, et al., J. Math. Biol. (2014).
19. A. V. Kolobov and M. B. Kuznetsov, Russ. J. Num. Anal. Math. Model. **28** (5), 471 (2013).
20. S. K. Stamatelos, E. Kima, A. P. Pathak, and A. S. Popel, Microvasc. Res. **91**, 8 (2014).
21. A. V. Kolobov, A. A. Polezhaev, and G. I. Solyanyk, in *Mathematical Modelling and Computing in Biology and Medicine*, Ed. by V. Capasso (2003), pp. 603–609.
22. A. V. Kolobov, V. V. Gubernov, and A. A. Polezhaev, Math. Model. Nat. Phenom. **6** (7), 27 (2011).
23. A. Giese, R. Bjerkvig, M.E. Berens, and M. Westphal, J. Clin. Oncol. **21**, 1624 (2003).
24. A. V. Gusev and A. A. Polejaev, Int J. Biochem. Cell Biol. **30** (11), 1169 (1998).
25. O. N. Pyaskovskaya, D. L. Kolesnik, A. V. Kolobov, et al., Exp. Oncol. **30**, 269 (2008).
26. J. J. Casciari, S. V. Sotirchos, and R. M. Sutherland, Cell Prolif. **25**, 1 (1992).
27. M. Xiu, S. M. Turner, R. Busch, et al., FASEB J. 20 (Meet. Abstr. Suppl.), A718 (2006).
28. F. Milde, M. Bergdorf and P. Koumoutsakos, Biophys. J. **95**, 3146 (2008).
29. A. H. Ko, A. P. Venook, E. K. Bergsland, et al., Cancer Chemother. Pharmacol. **66** (6), 1051 (2010).
30. S. Takano, E. Ishikava, K. Nakai, et al., OncoTargets and Therapy, **7**, 1551 (2014).

*Translated by E. Berezhnaya*